JOURNAL OF BACTERIOLOGY, Mar. 1996, p. 1386–1393 Vol. 178, No. 5
0021-9193/96/$04.00+0

Characterization of a Glutathione-Dependent Formaldehyde Dehydrogenase from *Rhodobacter sphaeroides*

ROBERT D. BARBER,[1] MARC A. ROTT,[2] AND TIMOTHY J. DONOHUE[1]*

Department of Bacteriology, University of Wisconsin-Madison, Madison, Wisconsin 53706,[1] and Department of Biology and Microbiology, University of Wisconsin-La Crosse, La Crosse, Wisconsin 54601[2]

Received 27 September 1995/Accepted 21 December 1995

Glutathione-dependent formaldehyde dehydrogenases (GSH-FDH) represent a ubiquitous class of enzymes, found in both prokaryotes and eukaryotes. During the course of studying energy-generating pathways in the photosynthetic bacterium *Rhodobacter sphaeroides*, a gene (*adhI*) encoding a GSH-FDH homolog has been identified as part of an operon (*adhI-cycI*) that also encodes an isoform of the cytochrome c_2 family of electron transport proteins (isocytochrome c_2). Enzyme assays with crude *Escherichia coli* extracts expressing AdhI show that this protein has the characteristic substrate preference of a GSH-FDH. Ferguson plot analysis with zymograms suggests that the functional form of AdhI is a homodimer of ~40-kDa subunits, analogous to other GSH-FDH enzymes. These properties of AdhI were used to show that mutations which increase or decrease *adhI* expression change the specific activity of GSH-FDH in *R. sphaeroides* extracts. In addition, expression of the presumed *adhI-cycI* operon appears to be transcriptionally regulated, since the abundance of the major *adhI*-specific primer extension product is increased by the *trans*-acting *spd-7* mutation, which increases the level of both isocytochrome c_2 and AdhI activity. While transcriptional linkage of *adhI* and *cycI* could suggest a function in a common metabolic pathway, isocytochrome c_2 (periplasm) and AdhI (cytoplasm) are localized in separate compartments of *R. sphaeroides*. Potential roles for AdhI in carbon and energy generation and the possible relationship of GSH-FDH activity to isocytochrome c_2 will be discussed based on the commonly accepted physiological functions of GSH-FDH enzymes in prokaryotes and eukaryotes.

Most organisms have the ability, by using various metabolic pathways, to generate both carbon and energy from the oxidation of a wide spectrum of substrates. The function of these metabolic pathways often requires the coordinated expression of specific enzymes for substrate oxidation and novel electron carriers to generate cellular energy from this substrate. To understand how different metabolic pathways provide cells with both carbon and energy, we are studying the regulation and function of energy-generating systems in the purple nonsulfur photosynthetic bacterium *Rhodobacter sphaeroides*.

While energy-generating pathways in *R. sphaeroides* have been extremely well analyzed from biochemical and bioenergetic standpoints (24), genetic analysis has uncovered the existence of unexpected electron transport proteins. For example, recent experiments have identified a *c*-type cytochrome, isocytochrome c_2, which allows *R. sphaeroides* Spd mutants to grow photosynthetically in the absence of cytochrome c_2, the normal electron donor to the light-oxidized reaction center complexes (29). While the function of isocytochrome c_2 as a photosynthetic electron carrier in Spd mutants has been confirmed both genetically (31) and biochemically (46), a physiological role for this protein in wild-type cells is not known. Because mutational and complementation analysis indicated that ~1.5 kb of DNA upstream of the isocytochrome c_2 structural gene (*cycI*) was required for synthesis of this alternative electron carrier, it was suggested that this region might contain additional open reading frames transcriptionally linked to *cycI* (31).

Our results provide biochemical and genetic evidence that a gene (*adhI*) upstream of *cycI* encodes a glutathione-dependent formaldehyde dehydrogenase (GSH-FDH; also known as class III alcohol dehydrogenase). GSH-FDH enzymes are a well-studied class of the alcohol dehydrogenase protein family that have been discovered in both prokaryotes and eukaryotes (9, 16, 17, 25, 28, 33, 39, 45). Unlike many alcohol dehydrogenase enzymes, GSH-FDH do not exhibit appreciable activity with short aliphatic alcohols (43). Instead, GSH-FDH enzymes catalyze the NAD-dependent oxidation of long-chain alcohols or hydroxylated fatty acids. Specifically, *S*-hydroxymethylglutathione (HMGSH), an adduct formed spontaneously by glutathione (GSH) and formaldehyde (HCHO) (reaction 1), is both the preferred in vitro and presumed in vivo substrate for GSH-FDH enzymes (22, 41) (reaction 2).

Reaction 1: HCHO + GSH ⟨**spontaneous**⟩ HMGSH
Reaction 2: HMGSH + NAD^+ ⟨**GSH-FDH**⟩ *S*-formylglutathione + NADH + H^+

In this way, GSH-FDH enzymes can participate either in catabolism of single-carbon substrates like methanol (28) or in detoxifying formaldehyde generated by oxidative demethylation of methylated compounds (18).

In this paper, we show that *R. sphaeroides* AdhI has a high degree of sequence similarity to GSH-FDH enzymes. Also, when AdhI is expressed in *Escherichia coli*, it has the enzymatic activity, subunit molecular weight, and oligomeric state typical of members of this family. Furthermore, we find that GSH-FDH activity in *R. sphaeroides* correlates with expression of the *adhI-cycI* operon. Indeed, the levels of a major *adhI-cycI* transcript are increased by the *trans*-acting *spd-7* mutation, which elevates the abundance of isocytochrome c_2 in Spd mutants (31). Finally, by localizing AdhI to the *R. sphaeroides* cytoplasm, we address the potential for metabolic interactions in carbon and energy generation between this GSH-FDH enzyme and the periplasmic electron carrier isocytochrome c_2.

* Corresponding author. Mailing address: Department of Bacteriology, University of Wisconsin-Madison, 1550 Linden Drive, Madison, WI 53706. Phone: (608) 262-4663. Fax: (608) 262-9865. Bitnet: DONOHUE@MACC.WISC.EDU.

TABLE 1. Bacterial strains and plasmids

Strain or plasmid	Description	Source or reference
R. sphaeroides		
Ga	*crtD*	Laboratory strain
CYCA65	*crtD* Δ*cycA*::Kan	4
CYCA65R7	*crtD* Δ*cycA*::Kan *spd-7*	29
ADHI1	*crtD* Δ*adhI*::ΩSp^r	This work
E. coli		
DH5α	*supE44* Δ*lacU169* (ϕ80 *lacZΔM15*) *hsdR178 recA1 endA1 gyrA96 thi-1 relA-1*	1
S17-1	C600::RP-4 2-(Tc::Mu) (Kn::Tn7) *thi pro hsdR hsdM*$^+$ *recA*	36
Plasmids		
pUC18	Ap^r	23
pUC19	Ap^r	23
pSUP202	Ap^r Tc^r Cm^r Mob$^+$ pBR325 derivative	36
pHP45Ω	Source of ΩSp^r cartridge	26
pMAR5	2.5-kb *Bam*HI-*Hin*dIII restriction fragment containing *adhI-cycI* operon cloned into pUC18 in the same orientation as P_{lac}	31
pJES1	2.0-kb *Sma*I restriction fragment containing ΩSp^r cartridge cloned into blunt *Bgl*II-*Sal*I sites of *adhI* in pMAR5	This work
pJES2	4.3-kb *Pvu*II restriction fragment containing *adhI*::ΩSp^r from pJES1 cloned into blunt *Eco*RI site of pSUP202	This work

MATERIALS AND METHODS

Bacterial strains, plasmids, and growth conditions. The bacterial strains and plasmids used in this work are listed in Table 1. *E. coli* strains were grown at 37°C in Luria-Bertani medium. *R. sphaeroides* strains were grown in Sistrom's minimal medium A (37) at 32°C. Filter-sterilized supplements were added as follows: ampicillin, 100 μg/ml; tetracycline, 1 μg/ml for *R. sphaeroides* and 10 μg/ml for *E. coli*; spectinomycin, 25 μg/ml; and isopropyl-β-D-thiogalactopyranoside (IPTG), 1 mM.

DNA sequence analysis. DNA sequencing with *Taq* DNA polymerase (Promega, Inc., Madison, Wis.) was performed as suggested by the manufacturer with deazanucleoside triphosphate reagent kits. Most of the DNA sequence was obtained with *lac*-specific primers and double-stranded derivatives of the pUC18 or pUC19 vector. Primers specific to *R. sphaeroides* DNA were used to complete the generation of double-stranded DNA sequence. A list of plasmids and internal primers used is available upon request. The DNA and subsequent protein sequences were analyzed with software from the Genetics Computer Group, Madison, Wis. (3). The DNA sequence from the *Bam*HI to *Sal*I restriction endonuclease sites (Fig. 1) has been appended to the previously submitted sequence of *cycI* (31) in the Genome Sequence Data Base (accession number L47326).

Construction of a defined *adhI* null mutant. To construct an *R. sphaeroides* strain containing an *adhI* null mutation, a 506-bp restriction fragment internal to the coding sequence (Fig. 1) was replaced with a spectinomycin resistance gene. Specifically, pMAR5 plasmid DNA was digested with *Bgl*II and *Sal*I to remove *adhI* coding sequences, and the resulting DNA was made blunt by addition of nucleotide triphosphates and DNA polymerase I large (Klenow) fragment (19). This DNA was ligated with a ~2.0-kb *Sma*I restriction fragment carrying an omega (Ω) cartridge containing a spectinomycin resistance gene (Sp^r). The resultant plasmid (pJES1) was digested with *Pvu*II to generate a ~4.3-kb restriction fragment containing the interrupted (*adhI*::ΩSp^r) gene. This *Pvu*II restriction fragment was cloned into a filled-in *Eco*RI site of pSUP202, a mobilizable suicide vector (36). The resulting plasmid, pJES2, was used to construct Δ*adhI* null alleles in different *R. sphaeroides* strains by homologous recombination (26). Genomic Southern blot analysis with both *adhI*- and Ω-specific probes confirmed that the *adhI* locus was interrupted in these strain constructs (data not shown).

Enzyme assays. Experiments measuring GSH-FDH activity were performed with crude cell extracts. Either *R. sphaeroides* or IPTG-induced *E. coli* cells were grown aerobically to late log-early stationary phase, harvested at 8,000 × *g*, and washed with 150 mM sodium phosphate buffer (pH 8.5). Cell pellets were stored at −20°C until the assay was performed. Prior to lysis, the thawed cell pellet was suspended in 5 ml of 150 mM sodium phosphate buffer (pH 8.5) containing 0.1% phenylmethylsulfonyl fluoride as a protease inhibitor. The cells were lysed by two passes through a French press cell at 18,000 lb/in^2, DNase was added to a final concentration of 5 μg/ml, and the lysate was incubated on ice for 30 min. Cell debris was removed by centrifugation at 10,000 × *g* for 15 min, and the supernatant was assayed for GSH-FDH activity (see below). Protein concentrations were determined by the sodium dodecyl sulfate (SDS) modification of the Folin-phenol method (21), with bovine serum albumin as a standard.

Assays for GSH-FDH activity with HMGSH as a substrate were performed as described by Uotila and Koivusalo (40) with the following modifications: the final concentration of sodium phosphate buffer (pH 8.5) was 150 mM, the final concentration of NAD was 1 mM, and 0.01 to 1 mg of crude cell extract protein was added. A typical assay with other potential GSH-FDH substrates included a volume of cell extract containing 0.1 to 1 mg of total protein, 150 mM sodium phosphate buffer (pH 8.5), 1 mM NAD as an electron acceptor, and an appropriate concentration of substrate (1 mM for long-chain [>5 aliphatic carbons] alcohols and acids, 0.2 M to 1 M for short-chain [<5 aliphatic carbons] alcohols).

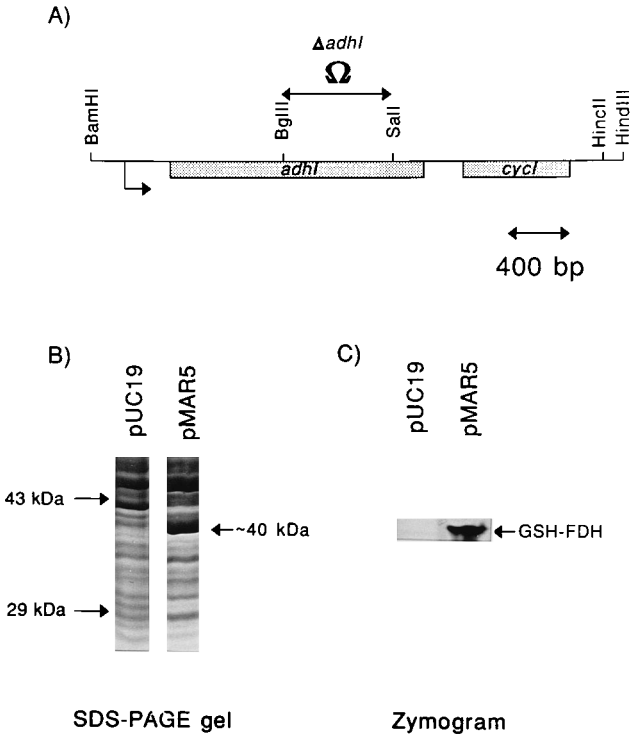

FIG. 1. Identification of the *adhI* gene product. (A) Summary of *adhI-cycI* genetic locus, depicting the orientation of genes with respect to the putative promoter region (arrow). The restriction map of the *adhI-cycI* operon shows the *Bgl*II and *Sal*I sites used in construction of the *adhI* null mutation (see Materials and Methods). (B) Protein-stained SDS-PAGE gel of crude extracts of *E. coli* cells harboring either pUC19 as a control or the *adhI* expression plasmid pMAR5. The migration positions of molecular size standards are shown on the left of the gel. (C) Activity stain gel analysis of crude extracts of *E. coli* cells harboring either pUC19 as a control or the *adhI* expression plasmid pMAR5. The protein species that stains in response to addition of HMGSH is noted by the arrow labeled GSH-FDH.

Enzyme activity was measured spectrophotometrically by the time-dependent reduction of NAD at room temperature in an SLM DW2000 spectrophotometer. One unit of GSH-FDH activity is defined as the amount of enzyme required to reduce 1 μmol of NAD per min.

Activity gel electrophoresis. Following native polyacrylamide gel electrophoresis, zymograms for GSH-FDH activity were modeled after previous work (42, 44). A half-volume of a loading solution, containing 40% (wt/vol) sucrose plus a trace of bromophenol blue, was added to an appropriate volume of cell extract prior to loading the gel. Proteins were separated on a 5% stacking gel and 10% separating gel with Tris-HCl buffer (pH 8.3) in the gel and Tris-glycine buffer (pH 8.8) in the electrode vessels, with an applied current of 10 to 20 mA per gel at 4°C for a minimum of 14 h.

Following electrophoresis, the gel was stained for GSH-FDH activity with a solution of 70 mM sodium phosphate buffer (pH 7.5), 500 mM KCl, 1.2 mM NAD, 4.8 mM formaldehyde, 1 mM glutathione, 0.4 mg of nitroblue tetrazolium per ml, and 0.03 mg of phenylmethylsulfate per ml with gentle shaking at 37°C. Enzyme activity was visualized in less than an hour, and the gel was rinsed in distilled water prior to photography.

Determination of the oligomeric state of active AdhI enzyme. Ferguson plot analysis was performed with a series of 5 to 10% native polyacrylamide gels (7, 10). The relative mobilities of carbonic anhydrase (29 kDa), bovine serum albumin (monomeric, 66 kDa; dimeric, 132 kDa), and β-amylase (215 kDa) were determined following Coomassie blue staining and normalized to the mobility of the bromophenol blue dye front. AdhI mobility on these identical gels was measured by activity stain and also normalized.

Localization of AdhI in *R. sphaeroides*. Fractionation of aerobically grown cells into cytoplasmic, periplasmic, cytoplasmic membrane, and outer membrane samples was performed by the method of Tai and Kaplan (38). Malate dehydrogenase, succinate dehydrogenase, and ascorbate-reducible cytochrome *c* were used as known markers for the cytoplasm, cytoplasmic membrane, and periplasm, respectively (20).

Primer extension analysis. RNA from aerobic *R. sphaeroides* cultures was prepared as previously described (47). An oligonucleotide (5′-ATTGACCTC CATGATCTCGA-3′) complementary to a region 42 nucleotides downstream of the *adhI* translational start codon was used for primer extension assays (Genosys, The Woodlands, Tex.). Primer (25 pmol) and RNA (15 μg) were hybridized at 45°C for 15 min; then, a solution of nucleotide triphosphates, reverse transcriptase, and actinomycin D was added and incubated for 30 min at 45°C. The reaction was stopped by adding a formamide-EDTA loading buffer. Samples were boiled prior to loading on a 6% denaturing polyacrylamide gel. Putative transcription initiation sites were mapped by comparison to DNA sequencing reactions generated with the same primer on an *adhI* template.

RESULTS

The *adhI* gene product is similar to GSH-FDH enzymes. Previous experiments suggested that ~1.5 kb of DNA upstream of *cycI* was required for expression of this gene (31). In addition, DNA sequencing had identified the carboxy terminus of a potential upstream open reading frame that ended 130 bp preceding the start of *cycI*. By sequencing the remainder of the 2.5-kb *Bam*HI-*Hin*dIII region containing *cycI*, we have identified a single upstream open reading frame of 1,128 bp (Fig. 1A). This potential open reading frame, designated *adhI*, has a putative ribosome-binding site (5′-GGGAGAG-3′) 5 nucleotides upstream of the translational start site and would encode a 376-amino-acid polypeptide with a predicted size of 42 kDa. To demonstrate the existence of the *adhI* gene product, we tested for the accumulation of a protein of the expected size in IPTG-treated *E. coli* cells containing a plasmid (pMAR5) with *adhI* cloned downstream of a pUC19 *lac* promoter. Under inducing conditions, the *adhI* gene on pMAR5 produced a protein of the expected size (~40 kDa) which was not present in *E. coli* cells containing pUC19 (Fig. 1B).

When the deduced AdhI protein sequence was compared with sequences in the SWISSPROT database, significant amino acid identity and similarity to members of the zinc- and NAD-dependent medium-chain alcohol dehydrogenase family were found. Previous work with zinc-dependent medium-chain alcohol dehydrogenases has identified amino acid sequences required for either structural or functional aspects of this enzyme family (13). The *adhI* gene product contains amino acid residues implicated as ligands for both the structural (C-100, C-103, C-106, and C-114) and catalytic (C-47, H-69, and C-182) zinc ions (Fig. 2). In addition, AdhI contains a typical Rossman fold sequence (residues 207-GLGGIG-212) indicative of a putative NAD^+ binding site, which would be expected from the use of pyridine nucleotides as a cofactor by many zinc-dependent alcohol dehydrogenases.

Despite overall sequence similarity to members of the alcohol dehydrogenase family, AdhI is distinct from several previously described bacterial zinc-dependent medium-chain alcohol dehydrogenases (represented in Fig. 2 by a *Zymomonas mobilis* alcohol dehydrogenase). The AdhI protein sequence has only 30% amino acid identity and 52% amino acid similarity with *Z. mobilis* alcohol dehydrogenase, values well below those obtained in comparisons between AdhI and human zinc-dependent medium-chain alcohol dehydrogenases (45% amino acid identity and 60% amino acid similarity [Fig. 2]).

In recent years, the mammalian zinc-dependent medium-chain alcohol dehydrogenases have been subdivided into classes I to V based on distinct biochemical properties, tissue distribution, and sequence determinants (2, 14, 15, 34). Among the mammalian alcohol dehydrogenase sequences, AdhI has the highest similarity to GSH-FDH (class III alcohol dehydrogenases), exhibiting 60% amino acid identity and 72% protein similarity to human GSH-FDH. During the preparation of this paper, a *Paracoccus denitrificans* GSH-FDH that has 89% amino acid identity and 95% amino acid similarity to *R. sphaeroides* AdhI was sequenced (Fig. 2).

Further support that AdhI is a bacterial GSH-FDH comes from inspection of specific sequence determinants that differentiate these enzymes from other zinc-dependent medium-chain alcohol dehydrogenases. For instance, the AdhI sequence contains a conserved arginine (residue 118 in Fig. 2) that is required for activity with some GSH-FDH substrates (6, 11). Furthermore, a comparison of amino acid sequence identity at positions in the predicted substrate-binding cleft (15) of the different classes of alcohol dehydrogenase (Fig. 2) indicates that AdhI is most similar to GSH-FDH enzymes. Overall, AdhI has 9 of 10 residues that are predicted to be conserved in the substrate-binding cleft of GSH-FDH enzymes. At most, AdhI has a 4 of 10 match when aligned with residues at the presumed substrate-binding cleft in other classes of eukaryotic zinc-dependent alcohol dehydrogenases.

AdhI exhibits characteristics typical of a GSH-FDH. Perhaps the most definitive property of GSH-FDH enzymes is substrate preference. GSH-FDH enzymes from various organisms oxidize long-chain aliphatic alcohols, long-chain hydroxylated fatty acids (i.e., 12-hydroxydodecanoic acid), and HMGSH in increasing order of preference (6, 9). However, unlike other classes of zinc-dependent alcohol dehydrogenases, GSH-FDH enzymes show little or no activity with short-chain aliphatic alcohols (43). To investigate if AdhI has the substrate preference characteristic of a GSH-FDH, enzyme assays were performed with crude extracts of *E. coli* cells containing the *adhI* expression plasmid pMAR5.

These enzyme assays showed that extracts of an *E. coli* strain harboring the *adhI* expression plasmid exhibited a substrate preference consistent with the production of a GSH-FDH (Table 2). NAD reduction with HMGSH (1 mM) as a substrate was dependent on *adhI* expression, since the GSH-FDH specific activity of these extracts was ~250-fold more than that present in extracts of a control *E. coli* strain lacking *adhI*. In addition, the crude extracts of *E. coli* cells prepared from the *adhI* expression strain exhibit significant in vitro NAD reduction with several other potential GSH-FDH substrates, although enzyme activity with these substrates is much lower then when HMGSH was provided (Table 2).

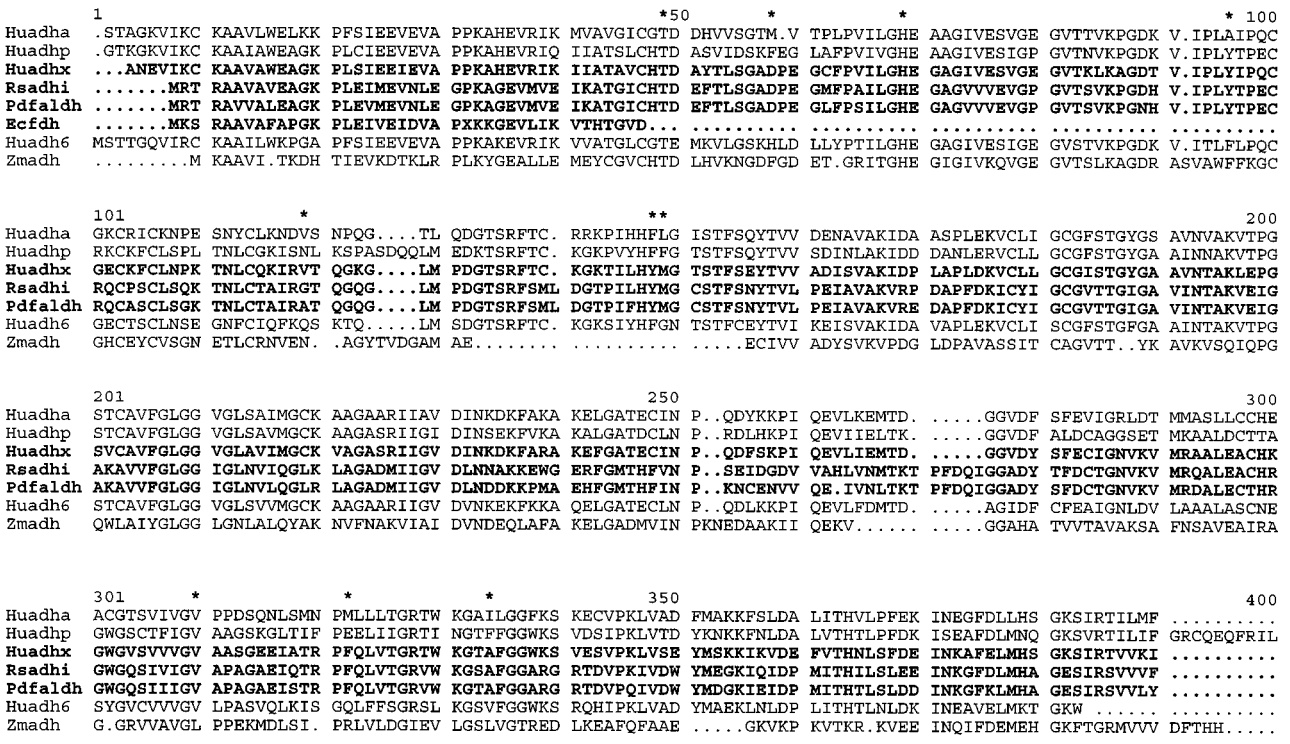

FIG. 2. Alignment of primary structures for various classes of alcohol dehydrogenases. Entries include human class I alcohol dehydrogenase α subunit (Huadha; accession number P07327), human class II alcohol dehydrogenase (Huadhp; P08319), human class III alcohol dehydrogenase (Huadhx; P11766), *R. sphaeroides* AdhI (Rsadhi; L47326), *P. denitrificans* glutathione-dependent formaldehyde dehydrogenase (Pdfaldh; U34346), *E. coli* N-terminal sequence of glutathione-dependent formaldehyde dehydrogenase (Ecfdh; A42015), human class V alcohol dehydrogenase (Huadh6; P28332), and *Z. mobilis* type I alcohol dehydrogenase (Zmadh; P20368). Residue numbering follows that of the human class V alcohol dehydrogenase. Gaps in sequences are marked by periods. Asterisks (*) denote residues predicted to comprise the substrate-binding cleft of the mammalian alcohol dehydrogenase family (15).

For example, enzyme activity was ~100-fold above that observed in the control with a long-chain hydroxylated acid (12-hydroxydodecanoic acid) as a substrate. Also, the use of long-chain alcohols (i.e., decanol and octanol) as substrates resulted in enzyme activity that was reproducibly six- to eightfold above that observed in the control extract. Finally, activity of about fivefold over the background was observed with butanol but only when the substrate was present at a high concentration (200 mM). In contrast, no significant activity over background was detected when various short-chain alcohols or aromatic alcohols (ethanol, propanol, isopropanol, isobutanol, hexanol, cyclohexanol, and benzyl alcohol) were used as substrates (data not shown). The activities reported for all substrates in Table 2 were dependent on NAD, since no AdhI-dependent substrate oxidation could be detected by using NADP as an electron acceptor under various pH conditions (data not shown). In summary, the analysis of AdhI's substrate preference indicates that it is a GSH-FDH enzyme.

TABLE 2. AdhI has the substrate profile of a GSH-FDH[a]

Substrate	Specific Activity	
	pMAR5	pUC19
HMGSH	2.500	0.010
12-HDA	0.211	0.002
Butanol	0.114	0.019
Decanol	0.024	0.003
Octanol	0.024	0.004
Various primary alcohols	>0.020	>0.020

Reaction: $R\text{-}CH_2OH + NAD^+ \longrightarrow R\text{-}\overset{H}{\underset{|}{C}}{=}O + NADH + H^+$

[a] Data are values obtained when AdhI is expressed from pMAR5 in *E. coli*. Specific activity is measured in micromoles of NAD reduced per minute per milligram of protein. Background activity in an *E. coli* strain containing pUC19 is listed on the right. These values represent the average activity from at least two independent cultures, with an estimated ±20% difference in activity observed between cultures. 12-HDA, 12-hydroxydodecanoic acid.

The oligomeric state of active GSH-FDH enzymes has previously been shown to be dimeric in both eukaryotes (27, 39) and *E. coli* (9). In contrast, the identified *P. denitrificans* GSH-FDH appears to be tetrameric (28). To analyze the oligomeric state of the functional AdhI protein, we used Ferguson plot analysis of activity-stained native polyacrylamide gels. Activity staining with HMGSH as a substrate revealed an enzyme specific to *E. coli* cells containing the *adhI* expression plasmid (Fig. 1C). When the migration of this GSH-FDH activity was analyzed on a series of native gels containing different polyacrylamide concentrations, the apparent size of this enzyme was ~75 to 80 kDa (Fig. 3). Thus, the enzymatically active form of *R. sphaeroides* AdhI appears to be dimeric when expressed in *E. coli.*

GSH-FDH activity in *R. sphaeroides* correlates with expression of the *adhI-cycI* operon. The spectrophotometric and electrophoretic assays used in analyzing *E. coli* cells expressing AdhI were employed to test for the presence of GSH-FDH

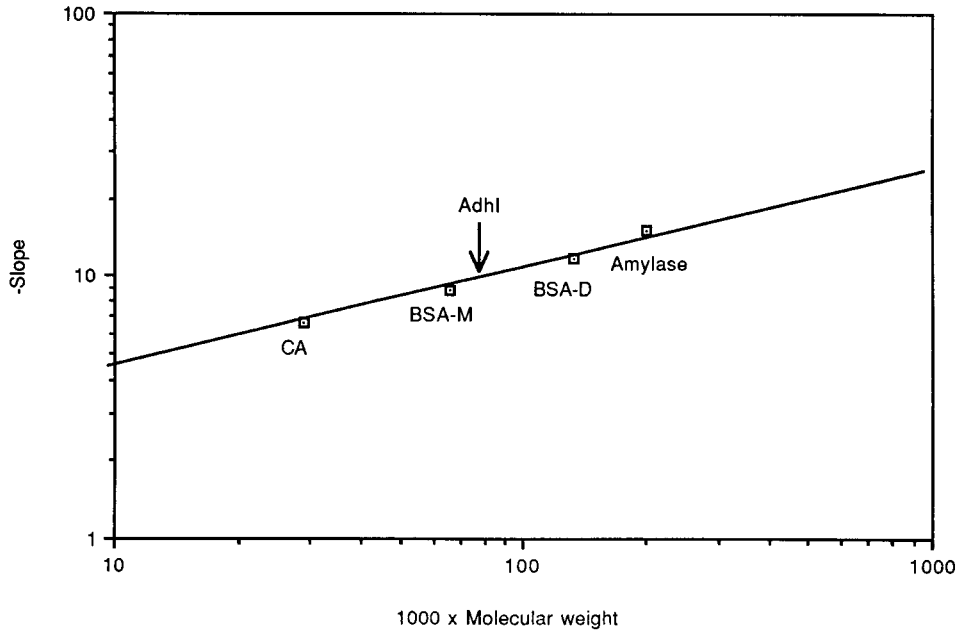

FIG. 3. Ferguson plot analysis of AdhI. The relative mobilities of carbonic anhydrase (29 kDa; CA), bovine serum albumin (monomeric, 66 kDa [BSA-M]; dimeric, 132 kDa [BSA-D]), β-amylase (215 kDa; amylase), and AdhI (monomeric, ~40 kDa) were determined and plotted against the percentage (5 to 10%) of polyacrylamide in each gel (data not shown). From these plotted data, a standard curve (shown) was constructed by deriving the slope for each standard protein and plotting negative slope versus molecular weight. From the standard curve, the approximate molecular mass (~80 kDa) of the active AdhI molecule (indicated by arrow) is derived.

activity in *R. sphaeroides*. Zymograms of crude extracts from wild-type *R. sphaeroides* demonstrated that an HMGSH-staining activity comigrates with the activity produced when *E. coli* harbors the *adhI* expression plasmid (Fig. 4). The comigration of AdhI in *R. sphaeroides* and *E. coli* extracts suggests that AdhI is also functional as a homodimer in *R. sphaeroides*. If the GSH-FDH activity present in wild-type cells was due to AdhI, then it should not be present in an *adhI* null mutant. Indeed, a Δ*adhI* strain (AdhI1) exhibits no GSH-FDH activity above background, and it lacks the ~80-kDa protein observed in zymograms with HMGSH used as a substrate (Fig. 4).

Furthermore, the apparent transcriptional linkage between

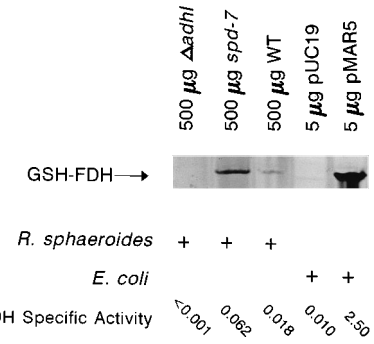

FIG. 4. Measurement and zymogram comparison of AdhI activity in *E. coli* and *R. sphaeroides* extracts. Extracts were prepared from aerobically grown *R. sphaeroides* ADHI1 (Δ*adhI*, lane 1), *R. sphaeroides* CYCA65R7 (*spd-7*, lane 2), *R. sphaeroides* Ga (wild type [WT], lane 3), *E. coli* containing pUC19 (lane 4), and *E. coli* containing pMAR5 (lane 5). Activity-stained proteins were detected by incubation with HMGSH as a substrate as described in Materials and Methods. GSH-FDH specific activity was measured for each strain in at least two independent culture extracts with HMGSH as a substrate. The specific activity is reported as micromoles of NAD reduced per minute per milligram of protein. Background activity of glutathione-independent formaldehyde oxidation was measured and subtracted for each assay.

adhI and *cycI* (31) predicts that GSH-FDH activity might increase in Spd mutants, which contain elevated levels of isocytochrome c_2. Indeed, CYCA65R7, a strain containing a *trans*-acting *spd-7* mutation that increases the level of isocytochrome c_2, contains about threefold more GSH-FDH activity than wild-type cells (Fig. 4). In summary, these experiments demonstrate that *R. sphaeroides* contains GSH-FDH activity that is dependent on expression of the *adhI* gene.

AdhI is a cytoplasmic protein. Since the apparent transcriptional linkage of *adhI* and *cycI* suggests that these two energy-generating proteins participate in a common metabolic pathway, we sought to determine if these proteins had the potential to interact directly. Previously, we have shown that isocytochrome c_2 is a periplasmic protein (29). However, *adhI* sequence analysis did not reveal any indication of a typical prokaryotic signal sequence. To evaluate the location of AdhI in *R. sphaeroides* cells, GSH-FDH activity was monitored in cells that had been fractionated into cytoplasmic, cytoplasmic membrane, periplasmic, and outer membrane fractions (38). For this analysis, proteins with known subcellular locations were used to assess the relative purity of cytoplasmic (malate dehydrogenase), cytoplasmic membrane (succinate dehydrogenase), and periplasmic (cytochrome *c*) fractions. When the distribution of AdhI activity (95% of the total activity is found in the cytoplasm) is compared with that of known marker proteins, it appears that AdhI is a cytoplasmic protein (Table 3). To ensure that this analysis was not compromised by the relatively low levels of enzyme activity present in wild-type cells, GSH-FDH activity was also localized in the *spd* mutant CYCA65R7, which contains increased AdhI activity. Again, AdhI appears to be cytoplasmic, because ~95% of GSH-FDH activity found in the *spd* mutant was present in the cytoplasm.

Levels of a specific *adhI-cycI* transcript are increased by the *spd-7* mutation. A simple explanation for the elevated levels of GSH-FDH activity in CYCA65R7 (Fig. 4 and Table 3) is that *adhI* and *cycI* constitute an operon whose transcription is in-

TABLE 3. AdhI is localized in the *R. sphaeroides* cytoplasm[a]

Fraction	Strain Ga (wild type)				Strain CYCA65R7 (*spd-7*)			
	MDH (U)	SDH (U)	Cyt *c* (pmol)	AdhI (U)	MDH (U)	SDH (U)	Cyt *c* (pmol)	AdhI (U)
Cytoplasm	5.5 (63)	ND[b]	160.0 (10)	204.5 (95)	7.7 (65)	9.0 (5)	104.9 (8)	932.8 (95)
Cytoplasmic membrane	0.3 (4)	341.0 (97)	224.0 (14)	7.3 (3)	0.2 (2)	176.0 (95)	289.8 (24)	24.2 (2)
Periplasm	2.6 (30)	10.0 (3)	1,156.6 (75)	4.2 (2)	3.6 (30)	ND	836.8 (66)	26.4 (3)
Outer membrane	0.2 (3)	ND	18.0 (1)	ND	0.3 (3)	ND	29.5 (2)	ND

[a] Values are the averages of at least two independent determinations and represent the total units of activity in 10^{11} cells. Numbers in parentheses represent the percentage of total activity in each fraction. One unit of malate dehydrogenase (MDH) activity is the amount of enzyme required to oxidize 1 μmol of NADH per min at 20°C. One unit of succinate dehydrogenase (SDH) activity is the amount of enzyme required to oxidize 1 nmol of phenazine methosulfate per min at 20°C. Values for cytochrome *c* (Cyt *c*) present in each fraction represent picomoles of total ascorbate-reducible cytochrome. One unit of GSH-FDH (AdhI) activity is the amount of enzyme required to reduce 1 nmol of NAD per min at 20°C.

[b] ND, none detected.

creased by the *spd-7* allele. Indeed, Northern (RNA blot) analysis with either *adhI*- or *cycI*-specific probes showed increased levels of a ~2.0-kb mRNA transcript in cells containing the *spd-7* mutation (data not shown). When primer extension analysis was used to evaluate if the observed increase in mRNA abundance reflects an effect of the *spd-7* allele at one or more *adhI-cycI* promoters, a major product in wild-type cells whose 5′ end maps 49 nucleotides upstream of the start of *adhI* translation was found (Fig. 5). A second primer extension product was detected 280 nucleotides upstream of the *adhI* translational start, but this transcript can only be observed following prolonged exposure (data not shown).

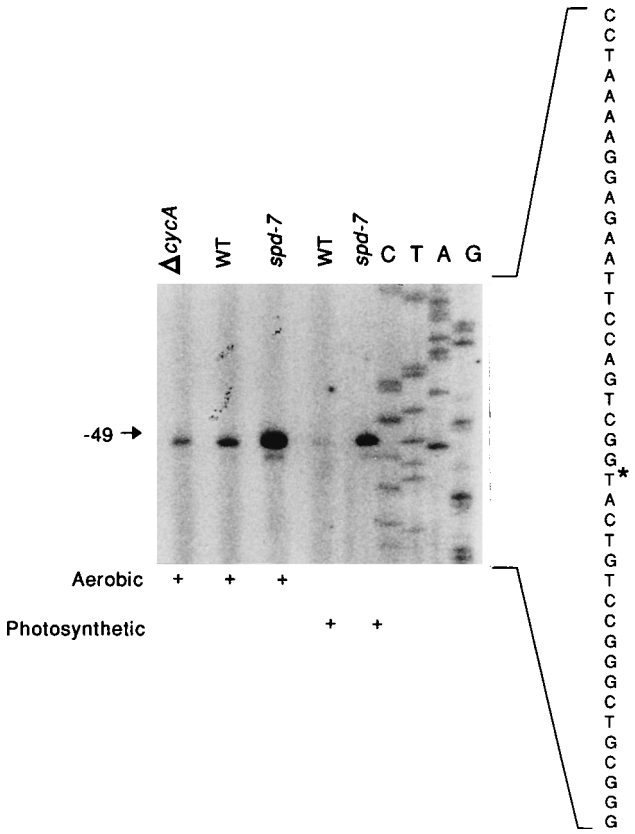

FIG. 5. Primer extension analysis of genomic *adhI*-specific mRNA products. The first three lanes contain primer extension products observed with mRNA obtained from aerobically grown cells of strains CYCA65 (Δ*cycA*), Ga (wild type [WT]), and CYCA65R7 (*spd-7*), respectively. Primer extension products from photosynthetically grown Ga and CYCA65R7 are in the next two lanes. The lanes marked C, T, A, and G indicate the DNA sequencing ladder used to map the mRNA 5′ end (indicated with an asterisk on the right). The mRNA 5′ end that maps 49 nucleotides upstream of the *adhI* translational start is noted with an arrow labeled −49.

It seems likely that the major primer extension product defines a primary transcript, since the region immediately upstream contains appropriately positioned hexamers (ATGC CG and TAAGGT) (see accession number L47326) with reasonable similarities (underlined) to consensus −35 and −10 elements often recognized by the major form of bacterial RNA polymerase holoenzymes. Transcription of the *adhI-cycI* operon does not seem to respond to the loss of cytochrome c_2, since the abundance of this primer extension product is similar in wild-type cells (wt) and a strain containing a Δ*cycA* mutation (Fig. 5). However, the level of this primer extension product is elevated in cells containing the *spd-7* mutation (Fig. 5). These results suggest that the increases observed in both the abundance of isocytochrome c_2 and the level of GSH-FDH activity caused by the *spd-7* allele are due to an increase in the level of a specific *adhI-cycI* transcript.

Additionally, these experiments reveal a slight but reproducible decrease in the major *adhI* primer extension product in both photosynthetically grown wild-type (wt) and *spd* mutant (*spd-7*) cells compared with aerobically grown cells (Fig. 5). The apparent reduction in the major *adhI-cycI* transcript under photosynthetic conditions in both wild-type (wt) and *spd-7* mutant cells supports previous studies showing that both strains contained slightly less isocytochrome c_2 in the absence of oxygen (30).

DISCUSSION

Previous genetic and molecular characterization of *R. sphaeroides cycI* suggested that the C terminus of a gene product encoded by a potential upstream open reading frame had significant similarity to proteins in the alcohol dehydrogenase family (31). In this work, we demonstrate that this upstream gene product, AdhI, has GSH-FDH activity. The apparent existence of an *adhI-cycI* operon and the increase in abundance of *adhI*-specific mRNA in cells containing the *trans*-acting *spd-7* allele suggest that AdhI might be required to generate energy under specific conditions in *R. sphaeroides.*

AdhI is a bacterial member of the GSH-FDH family. Until recently, the sequences for GSH-FDH enzymes had only been found in eukaryotes (8, 12, 33, 35, 45). Although GSH-FDH activity has been measured in several prokaryotes (16), sequence information on bacterial GSH-FDH enzymes includes only the N terminus of a potential *E. coli* homolog (9), a *P. denitrificans* GSH-FDH (28), and now *R. sphaeroides* AdhI. Sequence comparison of the two complete bacterial GSH-FDH enzymes shows that the *R. sphaeroides* and *P. denitrificans*

proteins have two insertions compared with their eukaryotic counterparts (Fig. 2). If one models *R. sphaeroides* AdhI on the crystallographic structure of a related class I alcohol dehydrogenase (5), a six-amino-acid insertion (positions 269 to 275) is predicted to be in a surface loop of the coenzyme-binding domain. A similar analysis suggests that a one-amino-acid insertion (position 140) is located in a reverse turn in the catalytic domain. Since these insertions might alter catalytic activity, it could be interesting to determine any potential consequences of these amino acid insertions on the function or structure of the bacterial enzymes. It will also be interesting to see if similar amino acid insertions are present when sequences of other bacterial GSH-FDH enzymes become available.

AdhI displays characteristic structural and functional properties of a GSH-FDH when the protein is expressed in *E. coli* (Table 2). For example, AdhI and GSH-FDH enzymes from various sources (6, 9) catalyze NAD-dependent oxidation of HMGSH, long-chain hydroxylated fatty acids, and long-chain alcohols in decreasing order of substrate preference. Additionally, the lack of significant NAD-dependent reduction by AdhI with various short-chain alcohols and aromatic alcohols is not surprising when one considers the relatively low activity of other GSH-FDH enzymes with these substrates. Furthermore, Ferguson plot analysis with zymograms predicts that AdhI is active as a dimer, similar to the *E. coli* (9) and eukaryotic (27, 39) GSH-FDH enzymes. This observation suggests that the two previously mentioned amino acid insertions in AdhI do not significantly alter the substrate profile or oligomeric state of this enzyme. However, the cause for the apparently atypical behavior of the *P. denitrificans* GSH-FDH as a tetramer (28) remains unclear without additional experiments.

GSH-FDH activity in *R. sphaeroides* correlates with expression of *adhI*. Analysis of three *R. sphaeroides* strains that exhibit various degrees of *adhI-cycI* operon expression shows that GSH-FDH activity correlates with AdhI synthesis. While there are reports of glutathione-dependent formaldehyde oxidation by extracts of members of the family *Rhodospirillaceae* (32), to our knowledge, the data in this work provide the first direct biochemical and genetic support for a GSH-FDH homolog in this or any other photosynthetic bacterium. The increase in *adhI* transcript levels in cells containing the *spd-7* mutation suggests that *adhI* transcription is controlled. However, more experiments are required to identify metabolic signals which might increase synthesis of AdhI in wild-type cells.

What is the role of GSH-FDH in *R. sphaeroides?* When our data are considered with reports of GSH-FDH homologs in prokaryotes and eukaryotes, it seems possible that these enzymes are present in a wide variety of biological systems. Despite their apparent ubiquity, defined physiological functions for GSH-FDH homologs have yet to be described in most organisms. In higher eukaryotes, GSH-FDH enzymes have been implicated in the oxidation of formaldehyde that can be generated by oxidative demethylation of one or more methylated compounds (18). In this role, GSH-FDH generates energy in the form of NADH and prevents a build-up of a toxic and highly reactive molecule, formaldehyde. Within the microbial world, GSH-FDH enzymes have been identified in both methylotrophic and nonmethylotrophic organisms. The recent report that a defined *P. denitrificans* GSH-FDH mutant fails to grow on methanol as a sole carbon source clearly implicates this enzyme in methylotrophic growth (28). However, enteric bacteria are not known to be methylotrophic, so the function of a GSH-FDH in *E. coli* and other such bacteria (9, 16) could extend beyond a role in methanol oxidation.

In considering a metabolic function for AdhI in *R. sphaeroides*, several pieces of evidence suggest that it is not required for growth of wild-type cells under typical laboratory conditions. First, primer extension analysis suggests that *adhI* transcription is low when wild-type cells are grown in a succinate-based minimal medium. In addition, AdhI activity is not required for viability in this medium, since the *adhI* null mutation described in this paper does not prevent growth by photosynthesis or respiration in the presence or absence of oxygen (data not shown). If, as we believe, the increase in *adhI-cycI* transcription in cells containing the *spd-7* allele indicates that expression of this operon is repressed in succinate-based minimal medium, then we might be able to identify conditions which increase operon expression because one or both of these gene products are required.

Are AdhI and isocytochrome c_2 involved in one or more metabolic pathways? The transcriptional linkage of *adhI* and *cycI* suggests that the corresponding gene products interact in a metabolic pathway, coupling substrate oxidation and NADH formation to energy generation in an electron transport chain. However, direct interactions between AdhI and isocytochrome c_2 seem unlikely, since GSH-FDH (cytoplasm) and isocytochrome c_2 (periplasm) are located in different subcellular compartments. Despite the different cellular locations, AdhI and isocytochrome c_2 could still function in the same metabolic pathway, either by interacting through one or more intermediate electron carrier molecule(s) or by acting at different steps in a common catabolic pathway. In this regard, inspection of the DNA sequence upstream of *adhI*, between *adhI* and *cycI*, and downstream of *cycI* does not reveal the presence of any other significant open reading frames. Thus, it would not appear that such hypothetical intermediate electron carriers are products of the *adhI-cycI* operon. Another possibility is that isocytochrome c_2 may be required to reduce light-oxidized reaction center complexes in photosynthetically growing cells using a specific carbon source that generates formaldehyde. Although the characterization of AdhI has not produced a clear physiological role for isocytochrome c_2, it has provided a series of specific questions that are currently being addressed.

ACKNOWLEDGMENTS

These studies were supported by competitive grant USDA 94-37306-0336 and UW Hatch grant WIS3766 to T.J.D.

We thank Eva Ziegelhoffer and Marjeta Urh for helpful discussions concerning Ferguson plot analysis. Also, we thank the P. Kiley laboratory for the protein standards used in this analysis.

REFERENCES

1. **Bethesda Research Laboratories.** 1986. BRL pUC host: *Escherichia coli* DH5αTM competent cells. Bethesda Res. Lab. Focus **8:**9–10.
2. **Danielsson, O., S. Atrian, T. Luque, L. Hjelmqvist, R. Gonzalez-Duarte, and H. Jornvall.** 1994. Fundamental molecular differences between alcohol dehydrogenase classes. Proc. Natl. Acad. Sci. USA **91:**4980–4984.
3. **Devereux, J. R., P. Haeberli, and O. Smithies.** 1984. A comprehensive set of sequence analysis programs for the VAX. Nucleic Acids Res. **12:**387–395.
4. **Donohue, T. J., A. G. McEwan, S. Van Doren, A. R. Crofts, and S. Kaplan.** 1988. Phenotypic and genetic characterization of cytochrome c_2 deficient mutants of *Rhodobacter sphaeroides*. Biochemistry **27:**1918–1925.
5. **Eklund, H., B. Nordstrom, E. Zeppezauer, G. Soderlund, I. Ohlsson, T. Boiwe, B. Soderberg, O. Tapia, and C. Branden.** 1976. Three-dimensional structure of horse liver alcohol dehydrogenase at 2.4 Å resolution. J. Mol. Biol. **102:**27–59.
6. **Engeland, K., J. Hoog, B. Holmquist, M. Estonius, H. Jornvall, and B. L. Vallee.** 1993. Mutation of Arg-115 of human class III alcohol dehydrogenase: a binding site required for formaldehyde dehydrogenase activity and fatty acid activation. Proc. Natl. Acad. Sci. USA **90:**2491–2494.
7. **Ferguson, K. A.** 1964. Starch-gel electrophoresis—application to the classification of pituitary proteins and polypeptides. Metabolism **13:**985–1002.
8. **Giri, P. R., J. F. Krug, C. Kozak, T. Moretti, S. J. O'Brien, H. N. Seuanez,**

and D. Goldman. 1989. Cloning and comparative mapping of a human class III (χ) alcohol dehydrogenase cDNA. Biochem. Biophys. Res. Commun. **164:**453–460.

9. **Gutheil, W. G., B. Holmquist, and B. L. Vallee.** 1992. Purification, characterization, and partial sequence of the glutathione-dependent formaldehyde dehydrogenase from *Escherichia coli*: a class III alcohol dehydrogenase. Biochemistry **31:**475–481.
10. **Hendrick, J. L., and A. J. Smith.** 1968. Size and charge isomer separation and estimation of molecular weights of proteins by disc gel electrophoresis. Arch. Biochem. Biophys. **126:**155–164.
11. **Holmquist, B., J. Moulis, K. Engeland, and B. L. Vallee.** 1993. Role of arginine 115 in fatty acid activation and formaldehyde dehydrogenase activity of human class III alcohol dehydrogenase. Biochemistry **32:**5139–5144.
12. **Hur, M., and H. J. Edenberg.** 1992. Cloning and characterization of the *ADH5* gene encoding human alcohol dehydrogenase 5, formaldehyde dehydrogenase. Gene **121:**305–311.
13. **Jornvall, H., B. Persson, and J. Jeffery.** 1987. Characteristics of alcohol/polyol dehydrogenases: the zinc-containing long-chain alcohol dehydrogenases. Eur. J. Biochem. **167:**195–201.
14. **Julia, P., J. Farres, and X. Pares.** 1987. Characterization of three isoenzymes of rat alcohol dehydrogenase: tissue distribution and physical and enzymatic properties. Eur. J. Biochem. **162:**179–189.
15. **Kaiser, R., B. Holmquist, B. L. Vallee, and H. Jornvall.** 1989. Characteristics of mammalian class III alcohol dehydrogenases, an enzyme less variable than the traditional liver enzyme class I. Biochemistry **28:**8432–8438.
16. **Kaulfers, P., and A. Marquardt.** 1991. Demonstration of formaldehyde dehydrogenase activity in formaldehyde-resistant *Enterobacteriaceae*. FEMS Microbiol. Lett. **79:**335–338.
17. **Koivusalo, M., and L. Uotila.** 1990. Glutathione-dependent formaldehyde dehydrogenase (EC 1.2.1.1): evidence for the identity with class III alcohol dehydrogenase, p. 305–313. *In* H. Weiner, B. Wermuth, and D. W. Crabb (ed.), Enzymology and molecular biology of carbonyl metabolism 3. Plenum Press, New York.
18. **Ling, K., and T. Tung.** 1948. The oxidative demethylation of monomethyl-L-amino acids. J. Biol. Chem. **174:**643–645.
19. **Maniatis, T., E. F. Fritsch, and J. Sambrook.** 1982. Molecular cloning: a laboratory manual. Cold Spring Harbor Laboratory Press, Cold Spring Harbor, N.Y.
20. **Markwell, J. P., and J. Lascelles.** 1978. Membrane-bound, pyrimidine nucleotide-independent L-lactate dehydrogenase of *Rhodopseudomonas sphaeroides*. J. Bacteriol. **133:**593–600.
21. **Markwell, M. A. K., S. M. Haas, L. L. Bieber, and N. E. Tolbert.** 1978. A modification of the Lowry procedure to simplify protein determination in membrane and lipoprotein samples. Anal. Biochem. **87:**206–210.
22. **Mason, R. P., and J. K. M. Sanders.** 1986. Formaldehyde metabolism by *Escherichia coli*: detection by *in vivo* ^{13}C NMR spectroscopy of *S*-(hydroxymethyl)glutathione as a transient intracellular intermediate. Biochemistry **25:**4504–4507.
23. **Messing, J.** 1979. A multipurpose cloning system based on single stranded DNA bacteriophage M13. Recomb. DNA Tech. Bull. **2:**43–48.
24. **Meyer, T. E., and T. J. Donohue.** 1995. Cytochromes, iron-sulfur, and copper proteins mediating electron transfer from the cyt bc_1 complex to photosynthetic reaction center complexes, p. 725–745. *In* R. E. Blankenship, M. T. Madigan, and C. E. Bauer (ed.), Anoxygenic photosynthetic bacteria. Kluwer Academic Publishers, The Netherlands.
25. **Patel, R. N., C. T. Hou, and P. Derelanko.** 1983. Microbial oxidation of methanol: purification of formaldehyde dehydrogenase from *Pichia* sp. NRRL-Y-11328. Arch. Biochem. Biophys. **221:**135–142.
26. **Prentki, P., and H. M. Krisch.** 1984. *In vitro* insertional mutagenesis with a selectable DNA fragment. Gene **29:**303–313.
27. **Ramaswamy, S., M. el-Ahmad, O. Danielsson, H. Jornvall, and H. Eklund.** 1994. Crystallization and crystallographic investigations of cod alcohol dehydrogenase class I and class III enzymes. FEBS Lett. **350:**122–124.
28. **Ras, J., P. W. Van Ophem, W. N. M. Reijnders, R. J. M. Van Spanning, J. A. Duine, A. H. Stouthammer, and N. Harms.** 1995. Isolation, sequencing, and mutagenesis of the gene encoding NAD- and glutathione-dependent formaldehyde dehydrogenase (GD-FALDH) from *Paracoccus denitrificans*, in which GD-FALDH is essential for methylotrophic growth. J. Bacteriol. **177:**247–251.
29. **Rott, M. A., and T. J. Donohue.** 1990. *Rhodobacter sphaeroides spd* mutations allow cytochrome c_2-independent photosynthetic growth. J. Bacteriol. **172:**1954–1961.
30. **Rott, M. A., J. Fitch, T. E. Meyer, and T. J. Donohue.** 1992. Regulation of a cytochrome c_2 isoform in wild-type and cytochrome c_2 mutant strains of *Rhodobacter sphaeroides*. Arch. Biochem. Biophys. **292:**576–582.
31. **Rott, M. A., V. C. Witthuhn, B. A. Schilke, M. Soranno, A. Ali, and T. J. Donohue.** 1993. Genetic evidence for the role of isocytochrome c_2 in photosynthetic growth of *Rhodobacter sphaeroides* Spd mutants. J. Bacteriol. **175:**358–366.
32. **Sahm, H., R. B. Cox, and J. R. Quayle.** 1976. Metabolism of methanol by *Rhodopseudomonas acidophila*. J. Gen. Microbiol. **94:**313–322.
33. **Sasnauskas, K., R. Jomantiene, A. Januska, E. Levediene, J. Lebedys, and A. Janulaitis.** 1992. Cloning and analysis of *Candida maltosa* gene which confers resistance to formaldehyde in *Saccharomyces cerevisiae*. Gene **122:**207–211.
34. **Satre, M. A., M. Zgombic-Knight, and G. Duester.** 1994. The complete structure of human class IV alcohol dehydrogenase (retinol dehydrogenase) determined from the *ADH7* gene. J. Biol. Chem. **269:**15606–15612.
35. **Sharma, C. P., E. A. Fox, B. Holmquist, H. Jornvall, and B. L. Vallee.** 1989. cDNA sequence of human class III alcohol dehydrogenase. Biochem. Biophys. Res. Commun. **164:**631–637.
36. **Simon, R., U. Priefer, and A. Puhler.** 1983. A broad host range mobilization system for *in vivo* genetic engineering: transposon mutagenesis in Gram negative bacteria. Bio/Technology **1:**784–791.
37. **Sistrom, W. R.** 1960. A requirement for sodium in the growth of *Rhodopseudomonas sphaeroides*. J. Gen. Microbiol. **22:**778–785.
38. **Tai, S. P., and S. Kaplan.** 1985. Intracellular localization of phospholipid transfer activity in *Rhodopseudomonas sphaeroides* and a possible role in membrane biogenesis. J. Bacteriol. **164:**181–186.
39. **Uotila, L., and M. Koivusalo.** 1979. Purification of formaldehyde and formate dehydrogenases from pea seeds by affinity chromatography and *S*-formylglutathione as the intermediate of formaldehyde metabolism. Arch. Biochem. Biophys. **196:**33–45.
40. **Uotila, L., and M. Koivusalo.** 1981. Formaldehyde dehydrogenase. Methods Enzymol. **77:**314–320.
41. **Uotila, L., and B. Mannervik.** 1979. A steady-state kinetic model for formaldehyde dehydrogenase from human liver. Biochem. J. **177:**869–878.
42. **Urakami, T., and K. Komagata.** 1981. Electrophoretic comparison of enzymes in gram negative methanol utilizing bacteria. J. Gen. Appl. Microbiol. **27:**381–403.
43. **Wagner, F. W., X. Pares, B. Holmquist, and B. L. Vallee.** 1984. Physical and enzymatic properties of a class III isozyme of human liver alcohol dehydrogenase: χ-ADH. Biochemistry **23:**2193–2199.
44. **Weaver, C. A., and M. E. Lidstrom.** 1985. Methanol dissimilation in *Xanthobacter* H4-14: activities, induction and comparison to *Pseudomonas* AM1 and *Paracoccus denitrificans*. J. Gen. Microbiol. **131:**2183–2197.
45. **Wehner, E. P., E. Rao, and M. Brendel.** 1993. Molecular structure and genetic regulation of *SFA*, a gene responsible for resistance to formaldehyde in *Saccharomyces cerevisiae*, and characterization of its protein product. Mol. Gen. Genet. **237:**351–358.
46. **Witthuhn, V. C., J. Gao, S. Hong, S. Halls, M. A. Rott, C. Wraight, A. R. Crofts, and T. J. Donohue.** Unpublished data.
47. **Zhu, Y. S., and S. Kaplan.** 1985. Effects of light, oxygen, and substrates on steady-state levels of mRNA coding for ribulose-1,5-bisphosphate carboxylase and light-harvesting and reaction center polypeptides in *Rhodopseudomonas sphaeroides*. J. Bacteriol. **162:**925–932.